Journal of Medicinal Chemistry

Article

pubs.acs.org/jmc

Dibenzosuberones as p38 Mitogen-Activated Protein Kinase Inhibitors with Low ATP Competitiveness and Outstanding Whole Blood Activity

Stefan Fischer,[†] Heike K. Wentsch,[†] Svenja C. Mayer-Wrangowski,[‡] Markus Zimmermann,[†] Silke M. Bauer,[†] Kirsten Storch,[†] Raimund Niess,[†] Solveigh C. Koeberle,[†] Christian Grütter,[‡] Frank M. Boeckler,[†] Daniel Rauh,[‡] and Stefan A. Laufer*[,†]

[†]Institute of Pharmacy, University of Tübingen, Auf der Morgenstelle 8, D-72076 Tübingen, Germany

[‡]Chemische Biologie, Fakultät Chemie, Technische Universität Dortmund, Otto-Hahn-Strasse 6, D-44227 Dortmund, Germany

Supporting Information

ABSTRACT: p38α mitogen-activated protein (MAP) kinase is a main target in drug research concerning inflammatory diseases. Nevertheless, no inhibitor of p38α MAP kinase has been introduced to the market. This might be attributed to the fact that there is no inhibitor which combines outstanding activity in biological systems and selectivity. Herein an approach to the development of such inhibitors on the basis of the highly selective molecular probe Skepinone-L is described. Introduction of a "deep pocket" moiety addressing the DFG motif led to an increased activity of the compounds. Hydrophilic moieties, addressing the solvent-exposed area adjacent to hydrophilic region II, conserved a high activity of the compounds in a whole blood assay. Combined with their outstanding selectivity and low ATP competitiveness, these inhibitors are very interesting candidates for use in biological systems and in therapy.

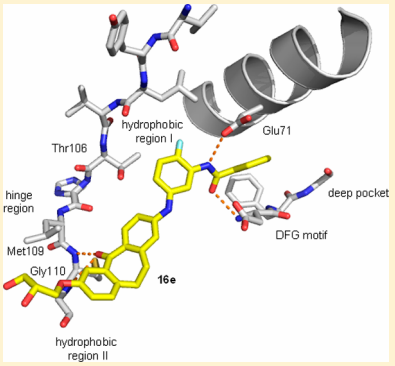

INTRODUCTION

Kinase inhibitors have proved to be drugs of major therapeutic and economic interest. As p38α MAP kinase is a key player in the regulation of inflammatory processes, it has been the target of many drug discovery and research efforts.[1]

Traditionally, the variety of considered applications covers a vast number of autoimmune diseases such as rheumatoid arthritis and inflammatory bowel disease.[2,3] Probably due to intolerable adverse effects of chronic application of many p38α MAP kinase inhibitors, attention has shifted to more acute inflammatory disorders, e.g., pulmonary diseases.[1] So far, no inhibitor of p38α MAP kinase has advanced to a final clinical stage.[4] Especially when dosed at high concentrations, many compounds showed toxic properties, partially due to off-target activity.[5−7] Consequently, there is a need for potent and selective p38α MAP kinase inhibitors with high efficacy, even when administered at a low dose. However, even compounds which proved to be potent in a biochemical kinase activity assay often showed poor activity, e.g., in whole blood assays,[8] which are most important to evaluate the potency of inhibitors in biological systems. The reason for this could be based on high intracellular concentrations of ATP competing with the inhibitor.

Therefore, research has focused on inhibitors which are less ATP competitive. These inhibitors change the conformation of the enzyme into an enzymatically inactive state and are therefore less easily displaced by ATP from the ATP binding site.[9,10] During binding of these inhibitors, the DFG motif is moved out of the so-called "deep pocket". As a result of this conformational change, the entrance to the ATP binding site is blocked by the activation loop of the enzyme (Figure 1).

Other unique features of this DFG-out binding mode are slow association and dissociation constants due to the necessary change of conformation. This structural transition increases the drug−target residence time and therefore improves efficacy of the inhibitors at low concentrations.[13,14]

The binding mode does not necessarily dictate selectivity of the compounds. Rather it has to be established by exploiting structural features of the kinase.[15]

There are two traditional approaches to the design of selective inhibitors of p38α MAP kinase. One of them is the glycine flip,[16] and the other one is the occupation of hydrophobic region I.[17]

Several inhibitors are able to form a second hydrogen bond to the hinge region of p38α MAP kinase after a conformational change of the enzyme (Figure 1A). This includes the rotation or flip of Gly110 and a conformational change of the adjacent Met109. Only 46 kinases show a glycine at this position. Amino acids with longer side chains are most probably not able to perform this flip. Affinity for the respective kinases should therefore be reduced.

Occupation of hydrophobic region I improves selectivity for p38α MAP kinase, as access to this region is only possible

Received: October 20, 2012
Published: December 27, 2012

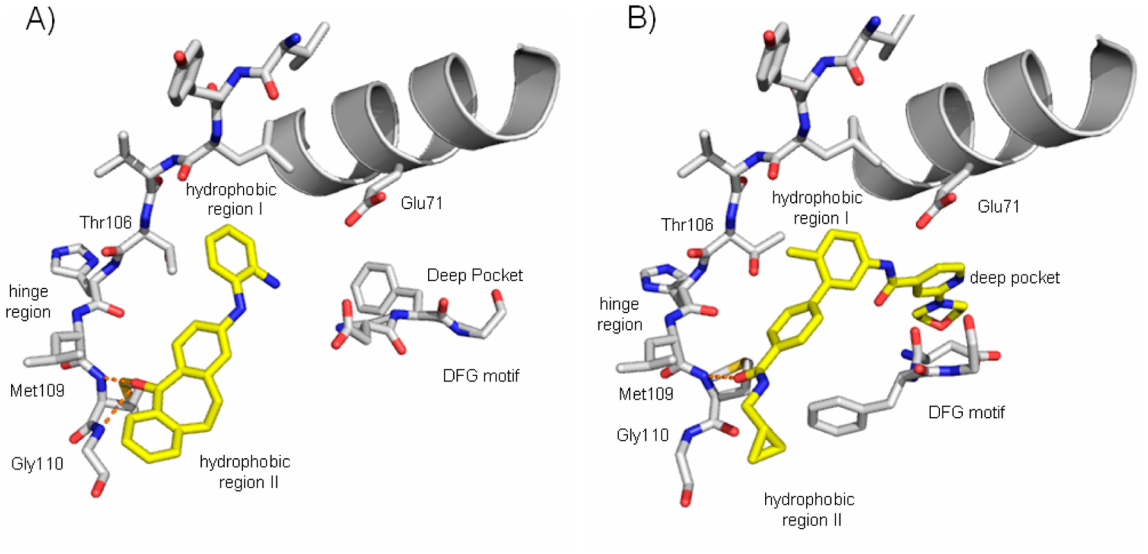

Figure 1. Crystal structures of p38α MAP kinase. (A) Crystal structure of p38α in complex with [(2-aminophenyl)amino]dibenzosuberone showing the DFG-in conformation. Phe169 of the DFG motif is located in the deep pocket (PDB code 3ZYA).[11] Two hydrogen bonds are formed to the hinge region by a flip of Gly110. (B) Crystal structure of p38α in complex with *N*-{4′-[(cyclopropylmethyl)carbamoyl]-6-methylbiphenyl- 3-yl}-2-morpholin-4-ylpyridine-4-carboxamide stabilizing the DFG-out conformation. Phe169 is located outside of the deep pocket (PDB code 3D83).[12].

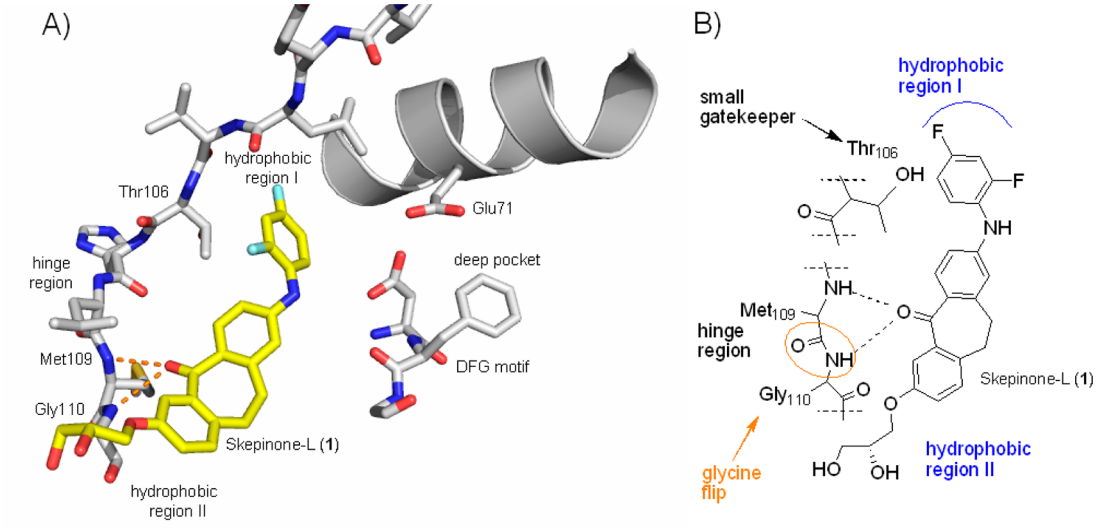

Figure 2. (*R*)-2-[(2,4-Difluorophenyl)amino]-7-(2,3-dihydroxypropoxy)-10,11-dihydrodibenzo[*a*,*d*]cyclohepten-5-one (**1**) in complex with p38α MAP kinase. (A) Crystal structure (PDB code 3QUE).[11] (B) Schematic binding mode.

because of the small gatekeeper residue Thr106 (Figure 1). Other kinases show a bulky methionine at this position displacing inhibitors with moieties directed into this region.

Recently, we reported another successful approach to selectivity: the design of very rigid inhibitors.[18] As protein kinases are quite flexible structures and undergo conformational changes during activation, there might be room for induced fits, together with flexible inhibitors. We were able to show that, by rigidization of kinase inhibitors, induced fits can be reduced and the selectivity of these inhibitors is therefore improved.[18]

Combination of these three selectivity features led to Skepinone-L (**1**),[11] which showed outstanding potency and selectivity (Figure 2). It was successfully used as a molecular probe in vitro and in vivo. In the present paper we discuss efforts to address the deep pocket by inhibitors which were derived from **1**. Introduction of novel hydrophilic moieties which are directed into the solvent-exposed area adjacent to hydrophilic region II conserved the whole blood activity of the modified compounds, most probably due to an improved solubility of the compounds. These modifications might be another step toward a drug in therapy of inflammatory diseases.

CHEMICAL RESULTS

Bristol-Meyers Squibb[19] and GlaxoSmithKline[12] addressed the deep pocket by adding amide moieties to the phenyl ring which occupies hydrophobic region I (Figure 3A). This approach was transferred to inhibitors developed by our group, showing a binding mode similar to that of compound **1** (Figure 3B).[20] As there were promising results, this procedure was applied to compound **1** as well. Furthermore, a novel dibenzosuberone scaffold was designed to easily introduce novel hydrophilic moieties, which should improve whole blood activity of the compounds.

dx.doi.org/10.1021/jm301539x | *J. Med. Chem.* 2013, 56, 241−253

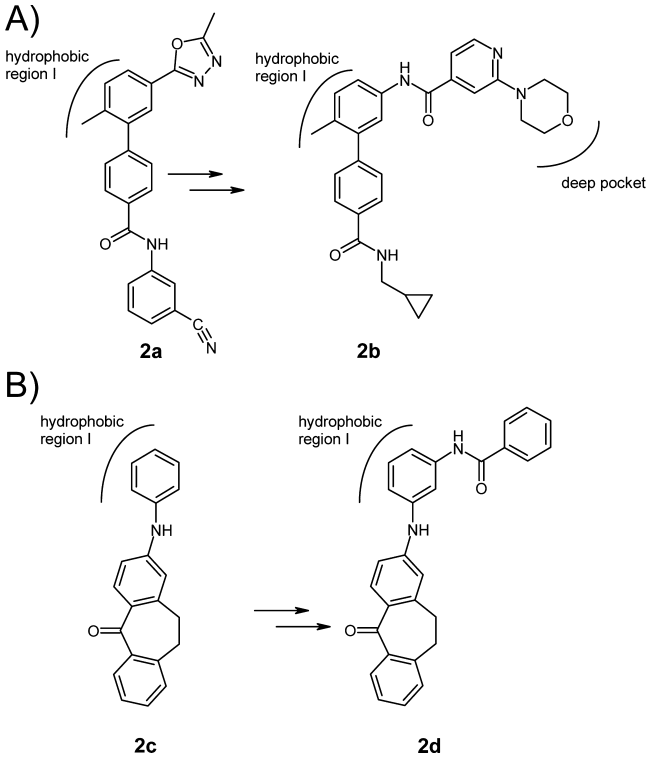

Figure 3. (A) Inhibitors developed by GlaxoSmithKline (**2a**) were able to address the deep pocket after addition of amide moieties directed into the deep pocket (**2b**). (B) A similar approach by our group (**2c** to **2d**).

Synthesis of the novel dibenzosuberone scaffold is described in Scheme 1. Compound **5** was synthesized according to a modified synthesis of Anzalone et al.[21] and coupled with 3-chlorobenzyl iodide (**6**). After hydrolysis of diester **7**, ring closure was performed by intramolecular Friedel–Crafts acylation. The scaffold **9** was subsequently converted to the respective alkyl amides **10a** and **10b**, Scheme 2).

Deep pocket moieties were synthesized according to Scheme 3 and coupled with **10a**, **10b**, and **15a–e** (synthesis is described by Koeberle et al.[18]) via Buchwald–Hartwig reaction (Scheme 4). Small anilines without any additional aryl carboxylic acid moieties were introduced the same way. Cleavage of the amide **16s** under acidic conditions yielded compound **17** (Scheme 5), which could now again be derivatized with amines and alcohols to the corresponding amides and esters. This way we were able to introduce functionalities which were unstable or incompatible with the conditions of the Buchwald–Hartwig reaction.

BIOLOGICAL RESULTS

Enzyme Assay and Inhibition of TNF-α Release in Whole Blood. All compounds were screened in two different enzyme-linked immunosorbent assays (ELISAs). The first one was a p38α MAP kinase activity assay, which used the isolated enzyme.[22] In the second one, the inhibition of lipopolysaccharide (LPS)-stimulated TNF-α (tumor necrosis factor-α) release in whole blood was analyzed.[23] As p38α MAP kinase is a key enzyme in the regulation of the proinflammatory enzyme TNF-α, its release can be used as an indicator of inhibitor potency.

At first a small series of compounds, quite similar to compound **1**, were prepared. By addition of benzoic acid moieties (**16a–16e**), which were suggested to presumably address the deep pocket by docking them into a related crystal structure, affinity for the enzyme was considerably improved (Table 1). This series suggested flexible hydrophilic moieties at position 7 (R4) which are directed into the solvent-exposed area adjacent to hydrophilic region II to be favorable for activity in the isolated p38α MAP kinase enzyme assay.

Nevertheless, inhibition of LPS-stimulated TNF-α release in whole blood was decreased (**1** vs **16e**), maybe due to high molecular mass and lipophilicity. Therefore, it was our primary aim to improve these parameters.

Exchange of the benzoic acid by tetrahydrofurancarboxylic acid was detrimental for affinity to the enzyme (**16b** vs **16f**). Altering the position of the fluoro atom reduced potency in whole blood even more (**16b** vs **16g**).

By exchanging the benzoic acid for heteroaromatic carboxylic acids (Table 2), affinity for the enzyme was improved. We obtained inhibitors with IC_{50} values below 1 nM by this approach (**16i, 16j, 16l**). The 3-thiophenecarboxylic acid derivative (**16i**) proved to be most potent compared to its 2-thiophene (**16j**) and 3-furan (**16h**) counterparts. Exchange of the ethylmorpholine (**16j**) moiety for a diol (**16l**) moiety did not alter the inhibitory potential. More importantly, the improvement in whole blood assays was even higher than that observed for the isolated p38α MAP kinase enzyme assay (**16d** vs **16i**). This can be ascribed to higher hydrophilicity of the heterocycles compared to phenyl. For the first time an improved whole blood activity compared to that of compound **1** could be detected (**1** vs **16i**).

Scheme 1. Synthesis of 8-Chloro-5-oxo-10,11-dihydro-5*H*-dibenzo[*a*,*d*]cycloheptene-3-carboxylic Acid (9)[a]

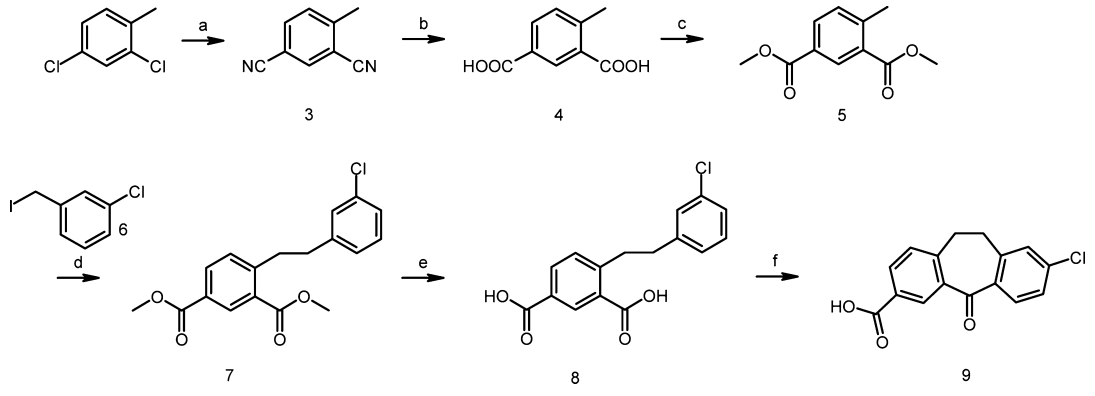

[a]Reagents and conditions: (a) CuCN, *N*-methylpyrrolidone, 200 °C, 7 d; (b) NaOH, diethylene glycol, 200 °C, 5 d; (c) H_2SO_4, MeOH, reflux, 29% for steps 1–3; (d) LDA, THF, −78 °C, 70%; (e) NaOH, MeOH, reflux, >95%; (f) (1) $SOCl_2$, DCM, reflux; (2) $AlCl_3$, rt, 98%.

dx.doi.org/10.1021/jm301539x | J. Med. Chem. 2013, 56, 241–253

Scheme 2. Synthesis of 10a and 10b[a]

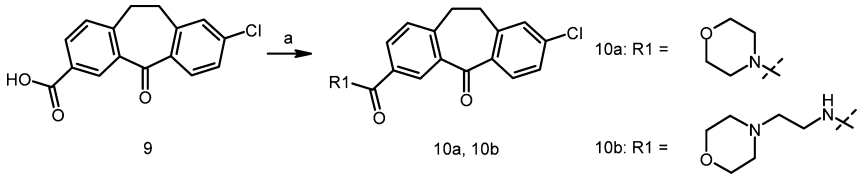

[a]Reagents: (a) (1) $SOCl_2$, DCM; (2) amino compound, Et_3N, DCM, >95%.

Scheme 3. Synthesis of Deep Pocket Moieties[a]

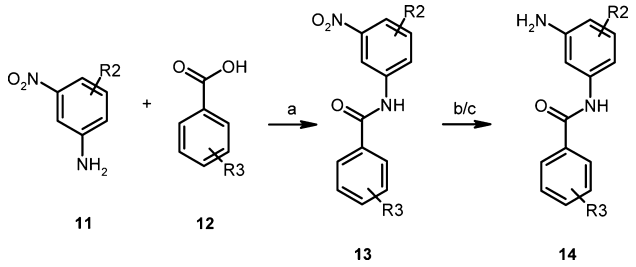

[a]Reagents and conditions: (a) (1) corresponding carboxylic acid, $(COCl)_2$, DCM or THF; (2) corresponding nitroaniline, Et_3N, DCM or THF, 12–33%; (b) H_2, Pd/C, ethyl actetate or MeOH, 32–95%; (c) $SnCl_2$, EtOH, 93–95%.

Scheme 4. Synthesis of 16a–u[a]

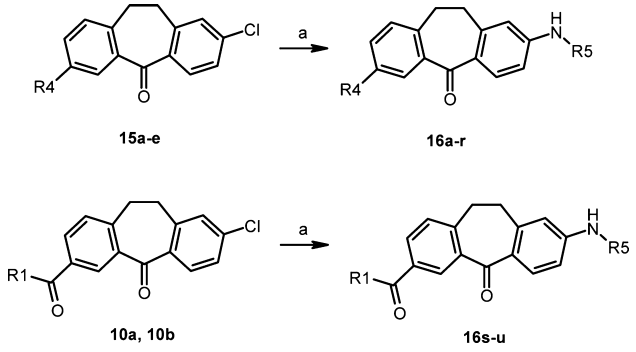

[a]Reagents: (a) $Pd(OAc)_2$, X-Phos, KO-*t*-Bu, toluene, *t*-BuOH, corresponding aniline (**14c,d,i,k,l–q**), 3–95%.

Scheme 5. Synthesis of Amides and Esters, Unstable under Buchwald–Hartwig Conditions[a]

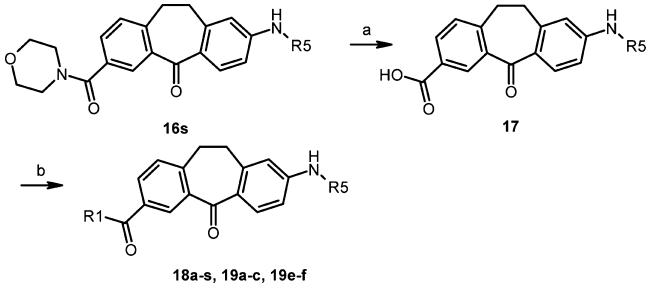

[a]Reagents and conditions: (a) HCl(concd), reflux, >95%; (b) various methods; see the Supporting Information.

Preliminary results[18] suggested an additional substitution of the phenyl which occupies hydrophobic region I to be beneficial. Therefore, the corresponding compounds were synthesized (Table 3). The addition of a methyl group (**16m** vs **16h**) and of a fluoro atom (**16p** vs **16d**) did not improve affinity for the enzyme, but potency in whole blood. Again, the 3-tetrahydrofurancarboxylic adic derivative **16n** showed a quite low inhibition (**16m** vs **16n**). Derivatives with an additional fluoro atom were more potent in whole blood than their methyl counterparts (**16n** vs **16o**). Again the derivative with the 3-thiophenecarboxylic acid (**16r**) was most potent.

As heterocycles in general and especially 3-thiophene might lead to toxic metabolites,[24] we had to provide backup structures. In the past, we had been successful in improving whole blood activity of dibenzosuberones by addition of a hydrophilic moiety at position 7 of the dibenzosuberone scaffold.[11] Therefore, we figured it possible to improve whole blood activity of the novel compounds by altering these hydrophilic moieties, yielding structures potent in whole blood using no heterocycles.

A dibenzosuberone scaffold was synthesized (Scheme 1) which showed a carboxylic acid at position 7. Using this functional group, new hydrophilic moieties could easily be introduced. We synthesized amides (Tables 4 and 5) and several esters (Table 6) to investigate interactions in and adjacent to hydrophobic region II with the aim of an improved whole blood performance. No deep pocket moieties were used for this optimization, but small moieties occupying only hydrophobic region I. This should ensure an easy and fast synthesis of multiple derivatives. The combination with deep pocket moieties should be performed afterward.

The carboxylic acid derivative **17** (Table 4) showed potency in the biochemical kinase activity assay comparable to that of the unsubstituted amide **18a**, but was inferior in the whole blood assay. This may be attributed to a reduced cell permeability of acid **17**, which may be deprotonated and therefore charged under physiological conditions.

A methyl-substituted amide (**18b**) already showed affinity for the enzyme comparable to that of compound **1**. No further increase in potency could be achieved by longer moieties featuring H-bond donor functions (**18d–18h**). Sterically hindered derivatives even led to less active compounds (**16s**, **18c**).

In the next series of compounds, derivatives with H-bond donor functions were synthesized (Table 5) including hydroxyl groups (**18i–18k**) and basic nitrogens (**16t**, **18l–18n**). While this strategy did not improve potency of the compounds in the isolated enzyme assay, activity in whole blood was increased, probably due to the higher hydrophilicity of the inhibitors. Furthermore, we synthesized a couple of compounds with derivatized amino acids. Again, the impact on enzyme activity was minor. Lipophilic derivative **18r** showed low activity in whole blood. Nevertheless, the quite lipohilic compound **18p** was extraordinarily potent, maybe due to a specific amino acid transporter, which recognized the inhibitor as a substrate.

Finally, a series of esters was synthesized (Table 6). The present derivatives were predominantly made to investigate structure–activity relationships in the solvent-exposed area adjacent to hydrophilic region II. Nevertheless, the use of esters,

dx.doi.org/10.1021/jm301539x | J. Med. Chem. 2013, 56, 241–253

Table 1. Biological Activity of Derivatives Featuring Deep Pocket Moieties and Different Hydrophilic Moieties at Position 7

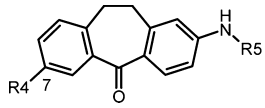

#	R4	R5	p38α (μM) IC_{50}± SEM[a]	TNF-α (μM) IC_{50}± SEM[b]
1	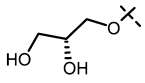	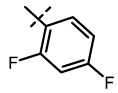	0.005[d] ± 0.002	0.04 ± 0.01
16a		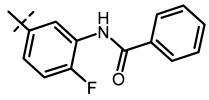	0.021 ± 0.002	4.1 ± 1.2
16b	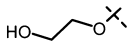	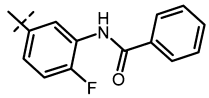	0.002 ± 0.000	2.4 ± 0.26
16c	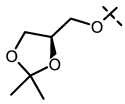	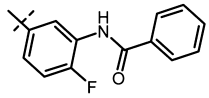	0.027 ± 0.003	0.45 ± 0.14
16d	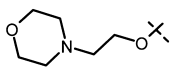	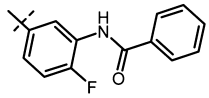	0.001 ± 0.000	0.26 ± 0.065
16e	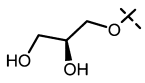	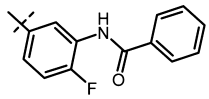	0.001 ± 0.000	0.28 ± 0.041
16f	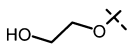	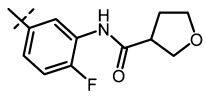	0.020 ± 0.000	1.5 ± 0.27
16g	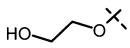	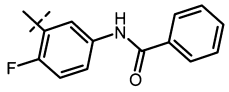	0.002 ± 0.000	9.0[c]

[a] $n = 3$. [b] $n = 2$. [c] $n = 1$. [d] $n = 6$.

especially as prodrugs, might be considered. In general, the ester derivatives showed a slightly increased affinity for the enzyme (**19a** vs **18b**, **19e** vs **18i**, **19f** vs **16t**) when compared to the corresponding amides. Consequently, the amides most likely do not act as H-bond donors. Otherwise, they would show superior potency. The inverted ester **19d** showed a decrease of potency, emphasizing the importance of the position and probably the electron density of the carboxyl group. Whole blood activity decreased for all ester compounds accordingly to their higher lipophilicity.

We combined both optimization strategies: novel hydrophilic moieties, improving activity in whole blood, and deep pocket moieties, which improved affinity for the enzyme. This approach led to **16u** (Table 7), which showed an IC_{50} value of 0.2 nM and was highly active in the whole blood assay, while the compound was rid of any heterocyclic structures which could be subject to metabolic pathways and lead to toxic intermediates.

Binding Mode of the Novel Compounds. Optimizing whole blood activity of the novel compounds was only one part of our work. Furthermore, we had to confirm our initial thesis that the deep pocket is accessible by introduction of novel moieties.

Recently, Simard et al.[10] developed FLiK (fluorescent labels in kinases), a fluorescence-based direct binding assay which is able to detect ligand-induced conformation changes in protein kinases,[25] including p38α MAP kinase. For this purpose, the enzyme is genetically altered and labeled with the environmentally sensitive fluorophore acrylodan. Binding of DFG-out ligands to the kinase domain of p38α induces conformational changes in the activation loop, moves the attached acrylodan to a

dx.doi.org/10.1021/jm301539x | J. Med. Chem. 2013, 56, 241−253

Table 2. Biological Activity of Derivatives Featuring Deep Pocket Moieties with Heterocyclic Structures

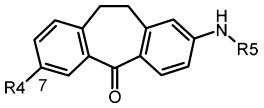

#	R4	R5	p38α (μM) IC_{50} ± SEM[a]	TNF- α (μM) IC_{50} ± SEM[b]
16h	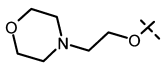	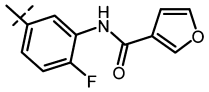	0.001 ± 0.000	0.11 ± 0.023
16i	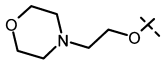	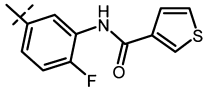	0.0003 ± 0.000	0.026 ± 0.003
16j	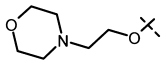	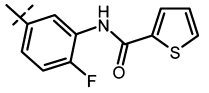	0.0007 ± 0.0001	0.095 ± 0.070
16k	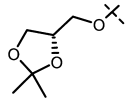	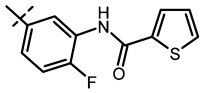	0.002 ± 0.000	0.30 ± 0.12
16l	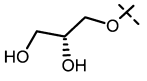	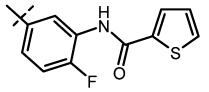	0.0007 ± 0.0001	0.042 ± 0.018

[a] $n = 3$. [b] $n = 2$.

more polar environment, and increases fluorescence emission at 514 nm, while emission at 468 nm is decreased. This way it is possible to determine both K_d values and K_{on} rates. Compound **16e** was subjected to this assay (Table 8).

For comparison, K_d and K_{on} of the known DFG-out binder 1-(5-*tert*-butyl-2-*p*-tolyl-2*H*-pyrazol-3-yl)-3-[4-(2-morpholin-4-ylethoxy)naphthalen-1-yl]urea (BIRB796) is shown in Table 8 too.[10] It was possible to determine a K_d value for **16e**, therefore suggesting that it induces a conformational change of the enzyme. Nevertheless, K_{on} of **16e** was 1000 times faster than that of BIRB796. We concluded that **16e** is able to stabilize the DFG-out conformation to some extent.

To confirm our observations, a cocrystallized structure of **16e** with the enzyme was examined by X-ray crystallography (Figure 4). The glycine flip is present and hydrophobic region I is occupied by the fluorophenyl moiety. The interaction geometry found in the crystal structure confirmed the ligand pose suggested initially by docking **16e** into crystal structure 3UVP.[20] The RMSD of the ligand's coordinates after structural alignment of both protein−ligand complexes was 0.91 Å (see the Supporting Information, SI-Figure 1). The crystal structure shows an active conformation of p38α, but the electron density indicates flexibility of the activation loop, and the inhibitor is therefore most probably able to stabilize the DFG-out conformation. The carbonyl oxygen of the amide is able to form a direct hydrogen bond to Asp168, which might be responsible for the stabilization of the DFG-out conformation observed in the fluorescence assay. Therefore, the results from both observations are coherent.

These results raised the question of whether the novel compound **16e** is less easily displaced by ATP than a traditional DFG-in binder. Although the inhibitor does stabilize the DFG-out conformation to some extent, the deep pocket is almost not addressed by the inhibitor.

Therefore, we modified our enzyme assay and applied increased concentrations of ATP. A DFG-out binder should show a reduced loss of potency when compared to classical DFG-in binders, if the amount of ATP is increased.

Even at high concentrations of ATP (300 μM, Table 9), **16e** is extremely potent. In contrast, the traditional DFG-in binder 4-{4-(4-fluorophenyl)-2-[4-(methylsulfinyl)phenyl]-1*H*-imidazol-5-yl}pyridine (SB203580) shows only a moderate inhibition at 300 μM ATP.

This experimental setup confirmed a low ATP competitiveness of compound **16e**. Competition with ATP might be reduced further by introduction of residues even longer than described herein, but whole blood activity would certainly suffer under these modifications.

Selectivity Screen. To confirm that our modifications of compound **1** were not detrimental with respect to selectivity, compounds **16u** and **18j** were screened against 451 kinases (see the Supporting Information, SI-Table 2).[26] As observed for compound **1** only p38α and p38β were inhibited in a relevant

dx.doi.org/10.1021/jm301539x | *J. Med. Chem.* 2013, 56, 241−253

Table 3. Biological Activity of Derivatives Featuring Deep Pocket Moieties with Additional Substitutions

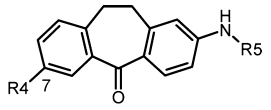

#	R4	R5	p38α (μM) IC_{50} ± SEM[a]	TNF- α (μM) IC_{50} ± SEM[b]
16m	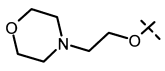	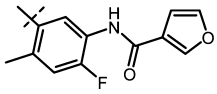	0.001 ± 0.000	0.032[c] ± 0.001
16n	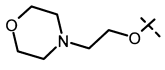	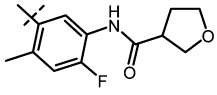	0.098 ± 0.005	0.57 ± 0.14
16o	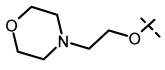	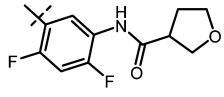	0.012 ± 0.002	0.15 ± 0.001
16p	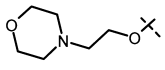	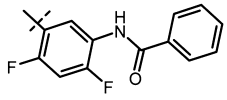	0.001 ± 0.000	0.22 ± 0.12
16q		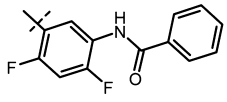	0.004 ± 0.000	0.29 ± 0.12
16r	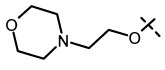	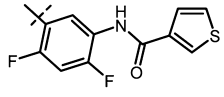	0.0005 ± 0.000	0.012[c] ± 0.008

[a] $n = 3$. [b] $n = 2$. [c] $n = 4$.

manner by **18j**. Compound **16u** additionally inhibited CSNK1E, but can still be considered as extremely selective.

CONCLUSION

In conclusion, we were able to design novel inhibitors of p38α MAP kinase based on **1** displaying subnanomolar IC_{50} values with respect to p38α MAP kinase and low nanomolar IC_{50} values with respect to TNF-α release in whole blood. The moiety occupying hydrophobic region I was optimized. Additional moieties which were intended to address the deep pocket were introduced. Crystallization experiments revealed that these moieties do not occupy the deep pocket, but form a hydrogen bond to the DFG motif. A fluorescence-based direct binding assay showed that the compounds are able to stabilize the DFG-out conformation to some extent. For further stabilization effects, longer moieties most probably have to be chosen. Novel hydrophilic moieties, which are directed toward the solvent-exposed area adjacent to hydrophilic region II, improved performance in the physiologically relevant human whole blood assay (**16u**, **18j**). Selectivity screens confirmed that none of these modifications were detrimental for selectivity (**16u, 18j**). The outstanding activity and low dependency on ATP concentrations of compound **16e** might mark the transition to a therapeutically relevant drug.

EXPERIMENTAL SECTION

General Information. All commercially available reagents and solvents were used without further purification. Flash chromatography was performed with a LaFlash system (VWR) and Merck silica gel (PharmPrep 60 CC 25−40 μm). Analytical HPLC analyses were run (method 1) on a Merck HPLC instrument (autosampler AS-2000, interface module D-6000, pump L-6200, detector L-4250) equipped with a LiChrospher RP18 column (5 μm) (Merck) or (method 2) on a LaChrome Ultra HPLC instrument (autosampler, interface module, oven L2300, pump L-216OU, detector diode array C-2455U) equipped with a Symmetry column (150 mm × 4.6 mm; 5 μm) (Waters). Melting points were determined with a Büchi B-545 melting point apparatus, and they were thermodynamically corrected. IR data were recorded with a Nicolet 380 FT-IR (ATR) spectrometer. Mass spectra were acquired on a Hewlett-Packard HP 6890 Series GC system equipped with an HP-5MS capillary column (0.25 μm film thickness, 30 m × 0.25 mm i.d.) (Hewlett-Packard) and an HP 5973 mass-selective detector (70 eV) (Hewlett-Packard). High-resolution measurements (Fourier transform ion cyclotron resonance) were obtained on a Bruker APEX II with electron spray ionization. ^{1}H NMR and ^{13}C NMR spectroscopies were performed on a Bruker Advance 200 MHz or a Bruker Ultra Shield 400 MHz spectrometer. The chemical shifts are reported in parts per million.

dx.doi.org/10.1021/jm301539x | J. Med. Chem. 2013, 56, 241−253

Table 4. Biological Activity of Amide Derivatives

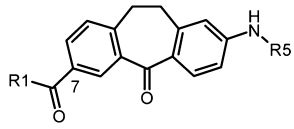

#	R1	R5	p38α (μM) IC_{50} ± SEM[a]	TNF- α (μM) IC_{50} ± SEM[b]
16s	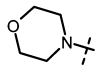	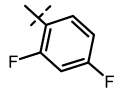	0.044 ± 0.012	39 @ 10μM[d]
17		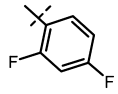	0.011[b] ± 0.004	0.49 ± 0.003
18a		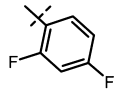	0.010 ± 0.002	0.019[e]
18b		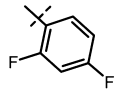	0.003 ± 0.000	0.037 ± 0.007
18c	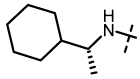	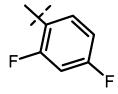	0.089 ± 0.009	7.6 ± 1.6
18d	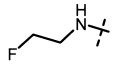	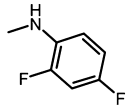	0.002 ± 0.000	0.083 ± 0.029
18e	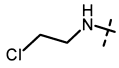	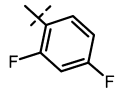	0.003 ± 0.000	0.064 ± 0.045
18f	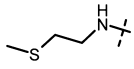	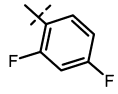	0.002 ± 0.000	0.036[a] ± 0.004
18g	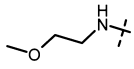	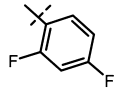	0.005 ± 0.000	0.054[c] ± 0.013
18h	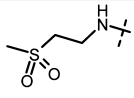	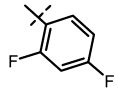	0.003 ± 0.000	0.050 ± 0.017

[a] $n = 3$. [b] $n = 2$. [c] $n = 4$. [d] Residual activity (μM) at a concentration of 10 μM. [e] $n = 1$.

The purity of tested compounds (>95%) was confirmed by HPLC analysis (see above, methods 1 and 2, and Supporting Information). Three compounds showed less than 95% purity (**16h**, 86%; **18b**, 92%; **19e**, 93%). The numbering of atoms for analytical purposes (e.g., NMR data) is defined in the Supporting Information for each compound as the direction of counting is different for some compounds compared to that proposed by IUPAC to maintain consistency.

General Procedure D. Chlorsuberone, aniline, X-Phos, KO-*t*-Bu, *t*-BuOH, and toluene are mixed in a three-necked flask under an argon atmosphere, followed by addition of $Pd(OAc)_2$. The mixture is heated to 90−100 °C for 15 min to 6 h. Complete conversion is determined by TLC. The reaction mixture is poured into water and extracted with ethyl acetate or diethyl ether. Solvents are removed in a rotary evaporator.

dx.doi.org/10.1021/jm301539x | *J. Med. Chem.* 2013, 56, 241−253

Table 5. Biological Activity of Amide Derivatives with Additional Hydrophilic Moieties

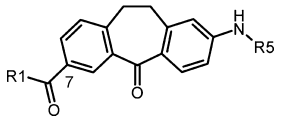

#	R1	R5	p38α (μM) IC_{50} ± SEM[a]	TNF- α (μM) IC_{50} ± SEM[b]
16t	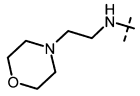	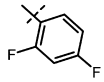	0.003 ± 0.000	0.029 ± 0.000[c]
18i	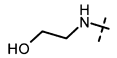	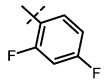	0.005 ± 0.000	0.027 ± 0.010
18j	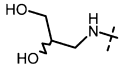	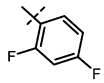	0.002 ± 0.000	0.029 ± 0.002
18k	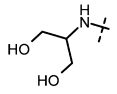	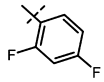	0.009 ± 0.002	0.017[c] ± 0.011
18l	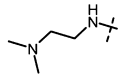	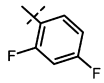	0.003 ± 0.001	0.018 ± 0.001
18m	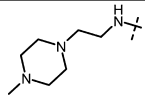	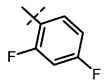	0.010 ± 0.002	0.027 ± 0.001
18n	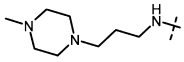	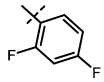	0.010 ± 0.002	0.019 ± 0.012
18o		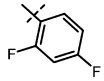	0.006 ± 0.000	0.095 ± 0.029
18p	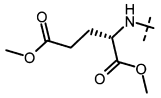	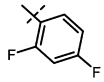	0.005 ± 0.000	0.018 ± 0.006[c]
18q	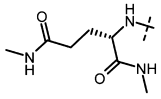	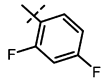	0.014 ± 0.001	0.064 ± 0.001
18r	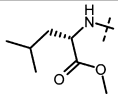	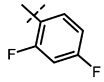	0.007 ± 0.001	0.46 ± 0.12
18s	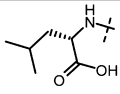	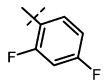	0.094 ± 0.001	n.i. @ 1μM[d]

[a] $n = 3$. [b] $n = 2$. [c] $n = 4$. [d] No inhibition at a concentration of 1 μM.

The crude product is purified by automated column chromatography (SiO_2). The product can be further purified by recrystallization.

*4-Methyl-isophthalonitrile (**3**).* A 200 g (2.23 mol) sample of CuCN in 100 g (0.62 mol) of 2,4-dichlorotoluene and 500 mL of *N*-methylpyrrolidone are mixed. The suspension is stirred for 7 days at 180 °C, cooled to 110 °C, and poured carefully into 1500 mL of NH_3 (25%). The mixture is extracted 10 times with ethyl acetate. The organic layers are separated by decantation. Ethyl acetate is removed in a rotary evaporator. The crude product is normally used in the next step without removal of the remaining *N*-methylpyrrolidone. The crude product can

dx.doi.org/10.1021/jm301539x | J. Med. Chem. 2013, 56, 241−253

Table 6. Biological Activity of Ester Derivatives

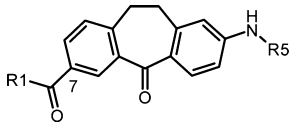

#	R1	R5	p38α (μM) IC_{50} ± SEM[a]	TNF- α (μM) IC_{50} ± SEM[b]
19a		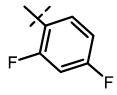	0.002 ± 0.000	0.16 ± 0.000
19b		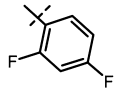	0.003 ± 0.000	0.27 ± 0.053
19c	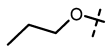	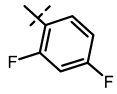	0.008 ± 0.001	0.22[a] ± 0.077
19d	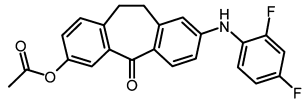		0.029 ± 0.020	2.3 ± 2.0
19e	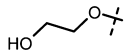	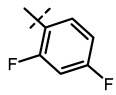	0.002 ± 0.000	0.21 ± 0.044
19f	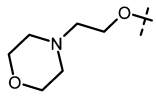	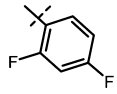	0.001 ± 0.000[b]	0.24 ± 0.008

[a] $n = 3$. [b] $n = 2$.

Table 7. Combination of Both Strategies: Novel Hydrophilic Moieties and Deep Pocket Moieties

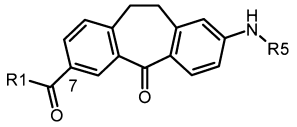

#	R1	R5	p38α (μM) IC_{50} ± SEM[a]	TNF- α (μM) IC_{50} ± SEM[b]
16u	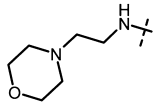	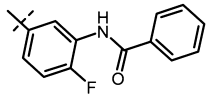	0.0002 ± 0.0000	0.031 ± 0.014

be purified further by recrystallization (ethyl acetate/hexane). The yield is determined after step 3 (compound **5**). ^{1}H NMR (DMSO-d_6) δ (ppm) (f = 200 MHz): 2.55 (s, 3 H, $-CH_3$), 7,68 (dd, 1H, J_1 = 0.6 Hz, J_2 = 8.1 Hz, C^5H), 8.06 (dd, 1 H, J_1 = 1.8 Hz, J_2 = 8.1 Hz, C^6H), 8.39 (d, 1 H, J = 1.8 Hz, C^2H). ^{13}C NMR (DMSO-d_6) δ (ppm) (f = 50 MHz): 20.7 ($-CH_3$), 110.2 (C^1), 113.6 (C^3), 116.6 (CN), 117.6 (CN), 131.9 (C^5), 136.7 (C^2), 136.7 (C^6), 147.6 (C^4).

*4-Methylisophthalic Acid (**4**).* A 90 g (633 mmol) sample of **3**, 120 g of NaOH (powder), 500 mL of diethylene glycol, and 30 mL of H_2O are mixed and refluxed for 5 d. Evaporated H_2O is replaced. The mixture is

dx.doi.org/10.1021/jm301539x | J. Med. Chem. 2013, 56, 241−253

Table 8. Kinetic Constants of 16e in Comparison to BIRB796

compd	K_d (nM)	K_{on} (M^{-1} s^{-1})
16e	17	1.1×10^6
BIRB796	12	4.3×10^3

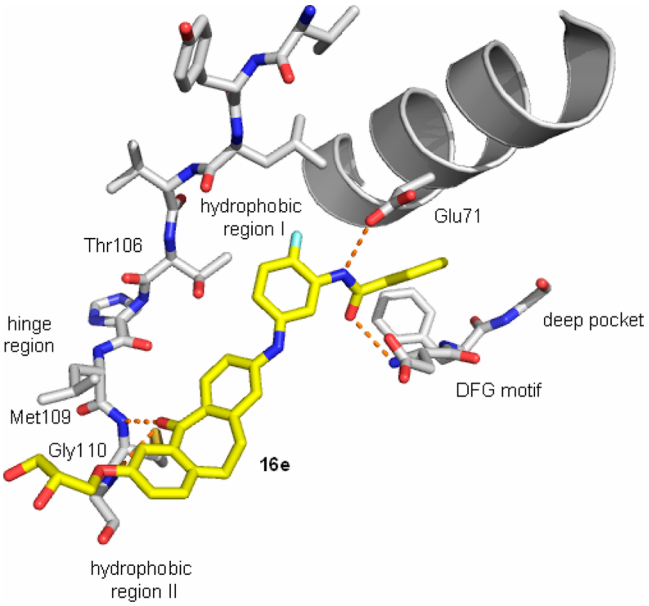

Figure 4. Crystal structure of **16e** in complex with p38α MAP kinase (PDB code 3UVQ). The DFG-in conformation is shown, but the electron density indicates flexibility of the activation loop.

Table 9. Connection of Inhibitory Activity and Concentration of ATP

	IC_{50}(p38α) ± SEM[a] (μM)	
compd	100 μM ATP	300 μM ATP
16e	0.001 ± 0.000	0.003 ± 0.000
SB203580	0.048 ± 0.004	0.273 ± 0.001

[a] n = 3.

poured into 1000 mL of H_2O, the product is precipitated using HCl(concd), and filtered. Remaining diethylene glycol is removed by washing the crude product with water at pH 1. The yellow powder is dried in vacuo. The yield is determined after step 3 (compound **5**). ^{1}H NMR (DMSO-d_6) δ (ppm) (f = 400 MHz): 2.58 (s, 3 H, $-CH_3$), 7.43 (d, 1 H, J = 7.8 Hz, C^5H), 7.97 (d, 1 H, J = 7.8 Hz, C^6H), 8.38 (s, 1 H, C^2H), 12.98 (s, 2 H, −COOH). ^{13}C NMR (DMSO-d_6) δ (ppm) (f = 100 MHz): 21.3 ($-CH_3$), 128.5 (C^1), 130.6 (C^3), 131.1 (C^5), 132.1 (C^2), 132.1 (C^6), 144.2 (C^4), 166.5 (−COO−), 167.8 (−COO−).

*4-Methylisophthalic Acid Dimethyl Ester (**5**).* A 55 g (305 mmol) sample of **4** is dissolved in 400 mL of methanol. A 10 mL volume of H_2SO_4 is added, and the mixture is refluxed for 6 h (monitored by TLC). Afterward the mixture is poured into water and extracted with ethyl acetate. The crude product is purified by automated column chromatography (SiO_2, petroleum ether (bp 60−90 °C)/ethyl acetate (95:5 to 90:10)) in 1 h. Yield: 29% (calcd for steps 1−3). ^{1}H NMR (DMSO-d_6) δ (ppm) (f = 400 MHz): 2.57 (s, 3 H, $-CH_3$), 3.71−3.99 (m, 6 H, $-COOCH_3$), 7.46 (d, 1 H, J = 8.1 Hz, C^5H), 7.99 (d, 1 H, J = 7.8 Hz, C^6H), 8.34 (s, 1 H, C^2H). ^{13}C NMR (DMSO-d_6) δ (ppm) (f = 100 MHz): 21.3 ($-CH_3$), 52.1 ($-COOCH_3$), 52.2 ($-COOCH_3$), 127.4 (C^1), 129.5 (C^3), 130.7 (C^5), 132.2 (C^2), 132.2 (C^6), 144.8 (C^4), 165.3 (−COO−), 166.3 (−COO−).

*4-[2-(3-Chlorophenyl)ethyl]isophthalic Acid Dimethyl Ester (**7**).* An 18 mL (45.0 mmol) sample of n-BuLi (2.5 M in hexane) is added dropwise during 15 min to a mixture of 6.35 mL (45.2 mmol) of diisopropylamine and 80 mL of THF at 0 °C. Stirring is continued for 15 min. A 5 g (24.0 mmol) sample of **5**, dissolved in 40 mL of THF, is slowly added at −78 °C. Stirring is continued for 1 h. Subsequently, 3-chlorobenzyl iodide (**6**) is added (during 30 min). The reaction mixture is allowed to warm to 0 °C during the night. After addition of NH_4Cl solution (satd), the product can be extracted using ethyl acetate. Solvents are removed in a rotary evaporator. The crude product is purified by automated column chromatography (SiO_2, petroleum ether (bp 60−90 °C)/ethyl acetate (95:5 to 90:10)) in 1 h. Yield: 70−75%. ^{1}H NMR (DMSO-d_6) δ (ppm) (f = 400 MHz): 2.85 (t, 2 H, J = 7.8 Hz, $-CH_2CH_2-$), 3.24 (t, 2 H, J = 7.8 Hz, $-CH_2CH_2-$), 3.87 (s, 6 H, $-CH_3$), 7,16 (d, 1 H, J = 7.3 Hz, $C^{6\prime}H$), 7.22−7.35 (m, 3 H, $C^{2\prime}/C^{4\prime}/C^{5\prime}$), 7.53 (d, 1 H, J = 8.1 Hz, C^3H), 8.04 (d, 1 H, J = 8.1 Hz, C^4H), 8.37 (s, 1 H, C^6H). ^{13}C NMR (DMSO-d_6) δ (ppm) (f = 100 MHz): 35.4 ($-CH_2CH_2-$), 36.4 ($-CH_2CH_2-$), 52.3 ($-CH_3$), 52.3 ($-CH_3$), 126.0 ($C^{6\prime}$), 127.1 ($C^{4\prime}$), 127.8 (C^5), 128.2 (C^3), 129.6 (C^1), 130.1 ($C^{2\prime}$), 130.9 (C^6), 131.8 ($C^{5\prime}$), 132.3 (C^4), 132.9 ($C^{3\prime}$), 143.7 ($C^{1\prime}$), 147.9 (C^2), 165.3 (−COO−), 166.3 (−COO−).

*4-[2-(3-Chlorophenyl)ethyl]isophthalic Acid (**8**).* A 6 g (18.0 mmol) sample of **7** is dissolved in 100 mL of methanol and 5 mL of H_2O. A 10 g sample of KOH is added and the resulting solution refluxed for 6 h (monitored by TLC). The reaction mixture is poured into water and extracted at pH 1 (HCl(concd)) using ethyl acetate. Solvents are removed in a rotary evaporator. Yield: >95%. ^{1}H NMR (DMSO-d_6) δ (ppm) (f = 400 MHz): 2.86 (t, 2 H, J = 7.9 Hz, $-CH_2CH_2-$), 3.26 (t, 2 H, J = 8.0 Hz, $-CH_2CH_2-$), 7.15−7.35 (m, 4 H, $C^{6\prime/2\prime/4\prime/5\prime}$), 7,46 (d, 1 H, J = 8.1 Hz, C^3H), 7.99 (d, 1 H, J = 7.8 Hz, C^4), 8.40 (s, 1 H, C^6H), 13.14 (s, 2 H, −COOH). ^{13}C NMR (DMSO-d_6) δ (ppm) (f = 100 MHz): 35.6 ($-CH_2CH_2-$), 36,5 ($-CH_2CH_2-$), 125.9 ($C^{6\prime}$), 127.0 ($C^{4\prime}$), 128.2 (C^3), 128.8 (C^5), 130.1 ($C^{2\prime}$), 130.5 (C^1), 131.4 (C^6), 131.5 ($C^{5\prime}$), 132,1 (C^4), 132,9 ($C^{3\prime}$), 144.0 ($C^{1\prime}$), 147.4 (C^2), 166.5 (−COO−), 167.9 (−COO−).

*8-Chloro-5-oxo-10,11-dihydro-5H-dibenzo[a,d]cycloheptene-3-carboxylic Acid (**9**).* A 6.5 g (21.3 mmol) sample of **8** is suspended in 150 mL of DCM and the suspension heated to reflux temperature. 8.5 mL (117.2 mmol) $SOCl_2$ are added dropwise. The reaction mixture is refluxed until a clear solution is visible. It might be necessary to add catalytic amounts of DMF. A 15.53 g (116.5 mmol) sample of $AlCl_3$ is added at 0 °C. After 20 min the mixture is poured onto ice, stirred for 30 min, and extracted with DCM. Solvents are removed in a rotary evaporator. Yield: 98%. ^{1}H NMR (DMSO-d_6) δ (ppm) (f = 400 MHz): 3.08−3.31 (m, 4 H, $-CH_2CH_2-$), 7.35−7.54 (m, 3 H, $C^{1/3/9}$), 7.90 (d, 1 H, J = 8.5 Hz, C^4H), 8.03 (dd, 1 H, J_1 = 1.9 Hz, J_2 = 7.8 Hz, C^8), 8.44 (d, 1 H, J = 1.8 Hz, C^6H), 13.0 (s, 1 H, −COOH). ^{13}C NMR (DMSO-d_6) δ (ppm) (f = 100 MHz): 33.7 (C^{11}), 34.2 (C^{10}), 127.1 (C^3), 129.6 (C^1), 129.6 (C^9), 130.7 (C^6), 131.7 (C^7), 132.7 (C^4), 133.3 (C^8), 136.6 (C^{4a}), 137.8 (C^{5a}), 137.9 (C^2), 144.7 (C^{11a}), 147,2 (C^{9a}), 166.8 (−COO−), 192.8 (C^5).

*2-Chloro-7-(morpholin-4-ylcarbonyl)-10,11-dihydrodibenzo[a,d]-cyclohepten-5-one (**10a**).* A 2.5 g (8.7 mmol) sample of **9** is dissolved in 10 mL of DCM, 3 mL (41.4 mmol) of $SOCl_2$ is added dropwise, and the solution is refluxed for 1 h. The reaction mixture is poured into a solution of 21.2 mL (243.3 mmol) of morpholine in 10 mL of DCM at 0 °C. Stirring is continued overnight at room temperature. Afterward the mixture is poured into water and extracted with ethyl acetate. Solvents are removed in a rotary evaporator. The yellow oil is washed with water and dried in vacuo. Yield: 3.0 g (97%). ^{1}H NMR (DMSO-d_6) δ (ppm) (f = 400 MHz): 3.09−3.22 (m, 4 H, $-CH_2CH_2-$), 3.51−3.83 (m, 8 H, morpholine), 7.15−7.30 (m, 3 H, $C^{1/3/9}H$), 7.46 (d, 1 H, J = 7.6 Hz, C^4H), 7.92 (d, 1 H, J = 8.6 Hz, C^8H), 7.97 (s, 1 H, C^6H). ^{13}C NMR (DMSO-d_6) δ (ppm) (f = 100 MHz): 34.6 (C^{10}), 34.7 (C^{10}), 66.9 (4 C, morpholine), 127.1 (C^3), 129.3 (C^1), 129.6 (C^9), 129.9 (C^6), 131.4 (C^8), 132.7 (C^4), 134.0 (C^{4a}), 136.2 (C^{5a}), 138.2 (C^7), 138.8 (C^2), 143.5 (C^{9a}), 143.7 (C^{11a}), 169.4 (−COO−), 192.9 (C^5).

*8-[[3-(Benzoylamino)-4-fluorophenyl]amino]-5-oxo-10,11-dihydro-5H-dibenzo[a,d]cycloheptene-3-carboxylic Acid (2-Morpholin-4-ylethyl)amide (**16u**).* The compound is synthesized according to general procedure D. A 0.37 g (0.93 mmol) sample of 8-chloro-5-oxo-10,11-dihydro-5*H*-dibenzo[*a*,*d*]cycloheptene-3-carboxylic acid (2-morpholin-4-ylethyl)amide (**10b**), 0.20 g (0.87 mmol) of *N*-(5-amino-2-fluorophenyl)benzamide (**14c**), 0.05 g (0.22 mmol) of $Pd(OAc)_2$, 0.14

dx.doi.org/10.1021/jm301539x | J. Med. Chem. 2013, 56, 241−253

g (0.29 mmol) of 2-(dicyclohexylphosphino)-2′,4′,6′-triisopropylbiphenyl, 0.40 g (3.6 mmol) of KO-*t*-Bu, 15 mL of toluene, and 3 mL of *t*-BuOH are reacted at 100 °C for 30 min. The reaction mixture is extracted with ethyl acetate. The crude product is purified by automated column chromatography (SiO_2, DCM/ethanol (95:5)). The product is further purified by recrystallization (ethyl acetate/hexane). Yield: 0.04 g (7%). HRMS (*m*/*z*): $[M + H]^+$ 593.255492 (calcd 593.255860). IR (ATR): 329, 1576, 1525, 1261, 1114, 861, 786, 706 cm^{-1}. ^1H NMR (DMSO-d_6) δ (ppm) (*f* = 200 MHz): 2.27−2.62 (m, 6 H + DMSO, $C^{2/6}_{\text{morpholinyl}}H/NCH_2CH_2NOC$), 2.99−3.21 (m, 4 H, $-CH_2CH_2-$), 3.24−3.48 (m, 2 H + H_2O, NCH_2CH_2NOC), 3.49−3.62 (m, 4 H, $C^{3/5}_{\text{morpholinyl}}H$), 6.86 (s, 1H, C^1H), 6.93−7.44 (m, 4 H, $C^{3/6\prime/5\prime/2\prime}H$), 7.47−7.62 (m, 4 H, $C^{4/3\prime\prime/5\prime\prime/4\prime\prime}H$), 7.86−8.06 (m, 4 H, $C^{9/2\prime\prime/6\prime\prime/8}H$), 8.32 (d, 1 H, *J* = 1.1 Hz, C^6H), 8.45−8.61 (m, 1 H, $-CONHCH_2-$), 8.89 (s, 1 H, −CONH−), 10.1 (s, 1H, −NH−). ^{13}C NMR (DMSO-d_6) δ (ppm) (*f* = 100 MHz): 33.8 (C^{10}), 35.5 (C^{11}), 36.4 ($-NCH_2CH_2NH-$), 53.2 (2 C, $C^{2/6}_{\text{morpholinyl}}$), 57.2 ($-NCH_2CH_2NH-$), 66.1 (2 C, $C^{3/5}_{\text{morpholinyl}}$), 112.6 ($C^3$), 113.9 ($C^1$), 116.2 (d, *J* = 20.4 Hz, $C^{5\prime}$), 118.1 (d, *J* = 6.5 Hz, $C^{6\prime}$), 118.2 (s, $C^{1\prime}$), 126.2 (d, 1 H, *J* = 13.8 Hz, $C^{3\prime}$), 127.2 (C^{4a}), 127.8 (2 C, $C^{2\prime\prime/6\prime\prime}$), 128.4 (2 C, $C^{3\prime\prime/5\prime\prime}$), 128.9 ($C^9$), 129.1 ($C^6$), 130.4 ($C^4$) 131.8 ($C^8$), 133.5 ($C^{4\prime\prime}$), 134.0 ($C^7$), 137.0 ($C^{5a}$), 137.1 ($C^{1\prime\prime}$), 138.9 ($C^2$), 144.5 ($C^{11a}$), 148.7 ($C^{9a}$), 150.9 (d, *J* = 241.4 Hz, $C^{4\prime}$), 165.5 (2 C, −CONH−), 190.3 (C^5).

■ ASSOCIATED CONTENT

Supporting Information

Kinetics of **16e**, crystallization and structure determination of p38α in complex with **16e**, analytical equipment and methods, synthetic procedures, ^1H NMR, ^{13}C NMR, HPLC, HRMS, and IR data, melting points, selectivity data of **16u** and **18j**, and molecular modeling. This material is available free of charge via the Internet at http://pubs.acs.org.

■ AUTHOR INFORMATION

Corresponding Author

*E-mail:stefan.laufer@uni-tuebingen.de. Phone: +49-7071-2972459. Fax: +49-7071-295037.

Notes

The authors declare no competing financial interest.

■ ACKNOWLEDGMENTS

We thank M. Goettert and K. Bauer for biological testing. D.R. is grateful for funds by the German federal state North Rhine Westphalia (NRW) and the European Union (European Regional Development Fund: Investing In Your Future) and the German Federal Ministry for Education and Research (NGFNPlus) (Grant No. BMBF 01GS08104). S.F. is grateful for advice and help of Annette Kuhn concerning the synthesis of the compounds.

■ ABBREVIATIONS USED

ATP, adenosine triphosphate; BuOH, butanol; CSNK1E, casein kinase 1 isoform ε; DCM, dichloromethane; ELISA, enzyme-linked immunosorbent assay; EtOH, ethanol; LDA, lithium diisopropylamide; LPS, lipopolysaccharide; MAP, mitogen-activated protein; MeOH, methanol; THF, tetrahydrofuran; TNF, tumor necrosis factor

■ REFERENCES

(1) Fischer, S.; Koeberle, S. C.; Laufer, S. A. p38α mitogen-activated protein kinase inhibitors, a patent review (2005−2011). *Expert Opin. Ther. Pat.* **2011**, *21*, 1843−1866.

(2) Regan, J.; Capolino, A.; Cirillo, P. F.; Gilmore, T.; Graham, A. G.; Hickey, E.; Kroe, R. R.; Madwed, J.; Moriak, M.; Nelson, R.; Pargellis, C. A.; Swinamer, A.; Torcellini, C.; Tsang, M.; Moss, N. Structure−activity relationships of the p38α MAP kinase inhibitor 1-(5-*tert*-butyl-2-*p*-tolyl-2*H*-pyrazol-3-yl)-3-[4-(2-morpholin-4-ylethoxy)naphthalen-1-yl]urea (BIRB 796). *J. Med. Chem.* **2003**, *46*, 4676−4686.

(3) Zhang, H.; Nei, H.; Dougherty, P. M. A p38 mitogen-activated protein kinase-dependent mechanism of disinhibition in spinal synaptic transmission induced by tumor necrosis factor-α. *J. Neurosci.* **2010**, *30*, 12844−12855.

(4) www.clinicaltrials.gov (accessed March 1, 2012), 2012.

(5) Cohen, S. B.; Cheng, T. T.; Chindalore, V.; Damjanov, N.; Burgos-Vargas, R.; Delora, P.; Zimany, K.; Travers, H.; Caulfield, J. P. Evaluation of the efficacy and safety of pamapimod, a p38 MAP kinase inhibitor, in a double-blind, methotrexate-controlled study of patients with active rheumatoid arthritis. *Arthritis Rheum.* **2009**, *60*, 335−344.

(6) Dominguez, C.; Powers, D. A.; Tamayo, N. p38 MAP kinase inhibitors: many are made, but few are chosen. *Curr. Opin. Drug Discovery Dev.* **2005**, *8*, 421−430.

(7) Hill, R. J.; Dabbagh, K.; Phippard, D.; Li, C.; Suttmann, R. T.; Welch, M.; Papp, E.; Song, K. W.; Chang, K. C.; Leaffer, D.; Kim, Y. N.; Roberts, R. T.; Zabka, T. S.; Aud, D.; Dal, P. J.; Manning, A. M.; Peng, S. L.; Goldstein, D. M.; Wong, B. R. Pamapimod, a novel p38 mitogen-activated protein kinase inhibitor: preclinical analysis of efficacy and selectivity. *J. Pharmacol. Exp. Ther.* **2008**, *327*, 610−619.

(8) Goldstein, D. M.; Gabriel, T. Pathway to the clinic: inhibition of P38 MAP kinase. A review of ten chemotypes selected for development. *Curr. Top. Med. Chem.* **2005**, *5*, 1017−1029.

(9) Rabiller, M.; Getlik, M.; Kluter, S.; Richters, A.; Tuckmantel, S.; Simard, J. R.; Rauh, D. Proteus in the world of proteins: conformational changes in protein kinases. *Arch. Pharm. (Weinheim, Ger.)* **2010**, *343*, 193−206.

(10) Simard, J. R.; Getlik, M.; Grutter, C.; Pawar, V.; Wulfert, S.; Rabiller, M.; Rauh, D. Development of a fluorescent-tagged kinase assay system for the detection and characterization of allosteric kinase inhibitors. *J. Am. Chem. Soc.* **2009**, *131*, 13286−13296.

(11) Koeberle, S. C.; Romir, J.; Fischer, S.; Koeberle, A.; Schattel, V.; Albrecht, W.; Grutter, C.; Werz, O.; Rauh, D.; Stehle, T.; Laufer, S. A. Skepinone-L is a selective p38 mitogen-activated protein kinase inhibitor. *Nat. Chem. Biol.* **2012**, *8*, 141−143.

(12) Angell, R. M.; Angell, T. D.; Bamborough, P.; Bamford, M. J.; Chung, C. W.; Cockerill, S. G.; Flack, S. S.; Jones, K. L.; Laine, D. I.; Longstaff, T.; Ludbrook, S.; Pearson, R.; Smith, K. J.; Smee, P. A.; Somers, D. O.; Walker, A. L. Biphenyl amide p38 kinase inhibitors 4: DFG-in and DFG-out binding modes. *Bioorg. Med. Chem. Lett.* **2008**, *18*, 4433−4437.

(13) Copeland, R. A.; Pompliano, D. L.; Meek, T. D. Drug-target residence time and its implications for lead optimization. *Nat. Rev. Drug Discovery* **2006**, *5*, 730−739.

(14) Simard, J. R.; Grutter, C.; Pawar, V.; Aust, B.; Wolf, A.; Rabiller, M.; Wulfert, S.; Robubi, A.; Kluter, S.; Ottmann, C.; Rauh, D. High-throughput screening to identify inhibitors which stabilize inactive kinase conformations in p38α. *J. Am. Chem. Soc.* **2009**, *131*, 18478−18488.

(15) Davis, M. I.; Hunt, J. P.; Herrgard, S.; Ciceri, P.; Wodicka, L. M.; Pallares, G.; Hocker, M.; Treiber, D. K.; Zarrinkar, P. P. Comprehensive analysis of kinase inhibitor selectivity. *Nat. Biotechnol.* **2011**, *29*, 1046−1051.

(16) Fitzgerald, C. E.; Patel, S. B.; Becker, J. W.; Cameron, P. M.; Zaller, D.; Pikounis, V. B.; O'Keefe, S. J.; Scapin, G. Structural basis for p38α MAP kinase quinazolinone and pyridol-pyrimidine inhibitor specificity. *Nat. Struct. Biol.* **2003**, *10*, 764−769.

(17) Lee, M. R.; Dominguez, C. MAP kinase p38 inhibitors: clinical results and an intimate look at their interactions with p38α protein. *Curr. Med. Chem.* **2005**, *12*, 2979−2994.

(18) Koeberle, S. C.; Fischer, S.; Schollmeyer, D.; Schattel, V.; Grutter, C.; Rauh, D.; Laufer, S. A. Design, synthesis, and biological evaluation of novel disubstituted dibenzosuberones as highly potent and selective inhibitors of p38 mitogen activated protein kinase. *J. Med. Chem.* **2012**, *55*, 5868−5877.

(19) Sack, J. S.; Kish, K. F.; Pokross, M.; Xie, D.; Duke, G. J.; Tredup, J. A.; Kiefer, S. E.; Newitt, J. A. Structural basis for the high-affinity binding of pyrrolotriazine inhibitors of p38 MAP kinase. *Acta Crystallogr., D: Biol. Crystallogr.* **2008**, *D64*, 705−710.
(20) Martz, K. E.; Dorn, A.; Baur, B.; Schattel, V.; Goettert, M. I.; Mayer-Wrangowski, S. C.; Rauh, D.; Laufer, S. A. Targeting the hinge glycine flip and the activation loop: novel approach to potent p38α inhibitors. *J. Med. Chem.* **2012**, *55*, 7862−7874.
(21) Anzalone, L.; Hirsch, J. A. Substitient effects on hydrogenation of aromatic rings: hydrogenation vs. hydrogenolysis in cyclic analogues of benzyl ethers. *J. Org. Chem.* **1985**, *50*, 2128−2133.
(22) Laufer, S.; Thuma, S.; Peifer, C.; Greim, C.; Herweh, Y.; Albrecht, A.; Dehner, F. An immunosorbent, nonradioactive p38 MAP kinase assay comparable to standard radioactive liquid-phase assays. *Anal. Biochem.* **2005**, *344*, 135−137.
(23) Linsenmaier, S. Entwicklung und optimierung von in vitro testverfahren zur evaluierung von hemmstoffen der p38α MAP kinase und JNK3. Ph.D. Thesis, Universität Tübingen, 2006.
(24) Walsh, J. S.; Miwa, G. T. Bioactivation of drugs: risk and drug design. *Annu. Rev. Pharmacol. Toxicol.* **2011**, *51*, 145−167.
(25) Simard, J. R.; Kluter, S.; Grutter, C.; Getlik, M.; Rabiller, M.; Rode, H. B.; Rauh, D. A new screening assay for allosteric inhibitors of cSrc. *Nat. Chem. Biol.* **2009**, *5*, 394−396.
(26) Ambit Biosciences Home Page. www.ambitbio.com (accessed March 1, 2012), 2012.